AD-A095 271 PURDUE UNIV LAFAYETTE IN DEPT OF GEOSCIENCES F/G 8/11
SYNTHETIC SEISMOGRAM MODELING.(U)
FEB 81 L W BRAILE N00014-75-C-0972
UNCLASSIFIED TR-1-81-ONR NL

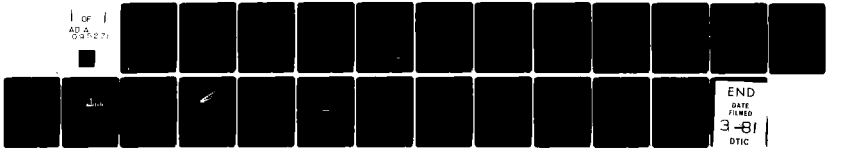

LEVEL II

12

DEPARTMENT OF GEOSCIENCES
PURDUE UNIVERSITY

Technical Report
for the
EARTH PHYSICS PROGRAM
OFFICE OF NAVAL RESEARCH
Contract No. N00014-75-C-0972

SYNTHETIC SEISMOGRAM MODELING

BY

Lawrence W. Braile

Technical Report No. ONR-1-81
Project Period 12/1/79-11/30/80
Report Date 2/05/81

Unclassified

SECURITY CLASSIFICATION OF THIS PAGE (When Data Entered)

REPORT DOCUMENTATION PAGE

READ INSTRUCTIONS BEFORE COMPLETING FORM

1. REPORT NUMBER: ONR-1-81	2. GOVT ACCESSION NO.: AD-A095 274
3. RECIPIENT'S CATALOG NUMBER	
4. TITLE (and Subtitle): SYNTHETIC SEISMOGRAM MODELING	5. TYPE OF REPORT & PERIOD COVERED: Technical 12/1/79-11/30/80
6. PERFORMING ORG. REPORT NUMBER: ONR-1-81	
7. AUTHOR(s): Lawrence W. Braile	8. CONTRACT OR GRANT NUMBER(s): N00014-75-C-0972
9. PERFORMING ORGANIZATION NAME AND ADDRESS: Department of Geosciences, Purdue University, West Lafayette, IN 47907	10. PROGRAM ELEMENT, PROJECT, TASK AREA & WORK UNIT NUMBERS
11. CONTROLLING OFFICE NAME AND ADDRESS: ONR Resident Representative, Ohio State University Research Center, 1314 Kinnear Road, Columbus, OH 43212	12. REPORT DATE: 2/81
	13. NUMBER OF PAGES
14. MONITORING AGENCY NAME & ADDRESS (if different from Controlling Office)	15. SECURITY CLASS. (of this report): Unclassified
	15a. DECLASSIFICATION/DOWNGRADING SCHEDULE: N/A

16. DISTRIBUTION STATEMENT (of this Report)

Unlimited

17. DISTRIBUTION STATEMENT (of the abstract entered in Block 20, if different from Report)

Approved for public release: distribution unlimited

18. SUPPLEMENTARY NOTES

Synthetic Seismograms, Seismic Modeling

19. KEY WORDS (Continue on reverse side if necessary and identify by block number)

20. ABSTRACT (Continue on reverse side if necessary and identify by block number)

Applications of synthetic seismogram modeling are the subject of two papers which have been or will be shortly published and which are reproduced in this report. Reflectivity method synthetic seismogram calculation utilizing a modified reflectivity code incorporating correct treatment of the free surface, non-zero depth of burial of the source, anelasticity (Q^{-1}) of the layered medium and realistic sources results in a useful modeling procedure which is capable of application to complex real-data situations. → cont.

DD FORM 1 JAN 73 1473 EDITION OF 1 NOV 65 IS OBSOLETE

S/N 0102-014-6601

SECURITY CLASSIFICATION OF THIS PAGE (When Data Entered)

cont.

The results of calculations for continental crustal and upper mantle structures yields information on the velocity and Q structure of the upper mantle and the wave propagation characteristics of several phase types including head waves, (such as P_n), guided wave phases ($\bar{P}$ and L_g) and wide angle reflections.

GEOPHYSICAL RESEARCH LETTERS, VOL. 7, NO. 12, PAGES 1029-1032, DECEMBER 1980

SEISMIC VELOCITY AND Q-STRUCTURE OF THE UPPER MANTLE LID AND LOW VELOCITY ZONE FOR THE EASTERN GREAT BASIN

K. H. Olsen,[1] L. W. Braile,[2] and P. A. Johnson[1]

[1]Geosciences Division, Los Alamos Scientific Laboratory, Los Alamos, New Mexico 87545
[2]Department of Geosciences, Purdue University, West Lafayette, Indiana 47907

Abstract. A 100-km-long record section of NTS explosions recorded in the eastern Snake River Plains ($7^{o}<\Delta<8^{o}$) shows the cusp of critical refractions from the steepened P velocity gradient at the bottom of the upper mantle LVZ. Synthetic seismograms calculated with a modified reflectivity program have been used to derive a regional velocity model of the upper mantle beneath the eastern Great Basin. The model suggests that observed very weak P_n arrivals are due to a slight negative velocity gradient below the Moho and that no high velocity mantle lid exists in this region.

Introduction

The seismic velocity versus depth structure of the upper mantle and lower crust beneath tectonically active areas of the western United States has been studied extensively for nearly 20 years. This has been possible because Nevada Test Site (NTS) underground explosions and western U.S. and Mexican earthquakes provide frequent seismic sources in an area well covered by seismograph stations. Compressional velocity distributions have mainly been determined by integrating the slope of the travel time curve, $dT/d\Delta$, using the Herglotz-Wiechert method. The required travel time (T) versus distance (Δ) data have been analysed from short-period recordings obtained along long-range profiles (Archambeau et al., 1969; Masse et al., 1972) and/or from apparent velocities measured directly across large seismic arrays (Johnson, 1967). Recently, availablility of high speed computers and development of sophisticated synthetic seismogram modeling techniques make it practical to fit the travel time and amplitude data by a trial and error procedure (Burdick and Helmberger, 1978; Wiggins and Helmberger, 1973). The important advantage of the synthetic seismogram method is that it makes optimum use of amplitude data and detailed waveform fitting to derive P velocity structure.

Many compressional and shear wave studies show that a major feature of the mantle structure beneath the western U.S. is a low velocity zone (LVZ) in the depth range between 60 and 300 km. It is well known that significant lateral variations in LVZ properties (thickness, depth, values of minimum S and P velocities, presence or absence of a lithospheric "lid," etc.) occur over distances of several hundred kilometers and perhaps to even finer scales (Burdick and Helmberger, 1978; York and Helmberger, 1973; Romanowicz and Cara, 1980). On the other hand, Burdick and Helmberger (1978) suggest mantle structure deeper than about 300 km is more uniform over a global scale and therefore amenable to modeling using widely spaced sources and seismograph stations if emphasis is placed on long period body wave arrivals at distances beyond 10°. Here we report on a record section of NTS explosions taken with matched short-period instruments having a sufficiently small station spacing (8 km) and yet long enough (~100 km) to identify at least three distinct (T, Δ) branches for P waves whose raypaths bottom in the uppermost mantle beneath a small area in east-central Nevada. Modeling of the arrival times, amplitudes, and waveforms using a reflectivity method synthetic seismogram program (Kind, 1978; Fuchs and Müller, 1971) enables us to perturb the generic western U.S. models into a crust-upper mantle model which gives fine details of the LVZ transition in this region.

Observations

Our observations are recordings of two NTS nuclear explosions obtained while our equipment was deployed in eastern Idaho during the Yellowstone-Snake River Plains (Y-SRP) cooperative seismic profiling experiment (Braile et al., 1979). Twelve special high-explosive shots plus blasts at two quarries were used as sources for crustal profiles in eastern Idaho and Yellowstone Park. Figure 1a shows the area of the Y-SRP experiment; Figure 1b indicates those stations that were recorded on an approximate radial line to two NTS explosions on September 27, 1978 (Table 1). Because RUMMY and DRAUGHTS explosion sites were within 3 km of each other, our observed record sections are nearly identical except DRAUGHTS amplitudes are about 1/4 RUMMY amplitudes. We discuss only the better signal-to-noise RUMMY seismograms.

Instrumentation consisted of 13 vertical component short-period (1 Hz natural frequency) seismometers. Ten of these were telemetered to a centrally located site and recorded on analog magnetic tape; the three southernmost instruments were recorded on portable smoked paper units and FM tape recorders. All records were digitized at 100 samples per second and filtered (0-3 Hz) for this analysis.

The reduced-time, true relative amplitude record section for the RUMMY explosion is displayed in Figure 2. Three separate compressional phases within the first four seconds are marked on Figure 2a; our reasoning in so identifying these arrivals is as follows:

(1) The very first arrivals with an apparent velocity of 7.8-7.9 km/s are so weak that they could easily be missed on initial inspection. From the Y-SRP refraction data, we determined that the M-discontinuity is 40 km below these stations and the mantle P_n velocity is close to 7.9 km/s. An enlarged view of the first 12 seconds is shown in Figure 2b where the consistency of the P_n arrivals across the spread is more apparent. These Snake River Plains seismic stations had quite low background noise so the implication is that a true headwave P_n arrival will rarely be seen at distances beyond 600 km in the western U.S., except from events of $m_b \geq 6$. In these SRP seismograms the ratio of the amplitudes of the P_n arrivals to those of the $\overline{P}$ phase is smaller than 0.005. (The $\overline{P}$ energy arrives at reduced times greater than 32 seconds so is not shown in Figure 2a). Other investigators (e.g., Hill, 1972, 1973) have commented that P_n energy at these distances is probably very

Paper number 80L1475.

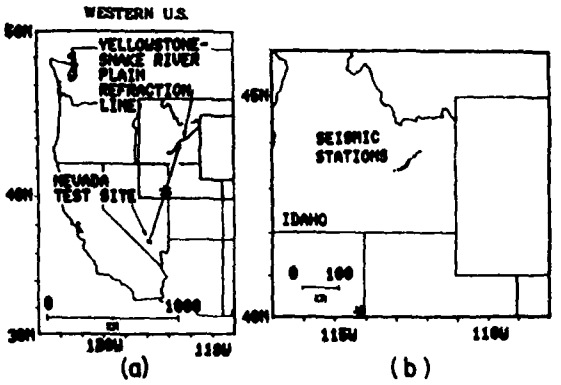

Figure 1. (a) Location map of the western U.S. with relative positions of the Nevada Test Site and the Y-SRP refraction line. (b) Enlargement showing seismic stations in Idaho used for the September 27 observations. Asterisk denotes the approximate area in the Great Basin for mantle ray turning points from NTS explosions.

weak and that care must be taken when attempting to extend the P_n branch during long range refraction profiling.

(2) Following P_n by about three seconds are stronger arrivals also having apparent velocities close to 8 km/s. A striking feature of Figure 2a is that beyond 780 km the amplitude of the second arriving phase increases rapidly with distance and the dominant frequency is noticably lower ($\sim$0.6 Hz) than the frequencies for Δ<780 km and for the P_n phase (both $\sim$1.6 Hz). This qualitative observation strongly suggests that the rapid increase of the low frequency phase for Δ< 780 km is a manifestation of a critical distance effect and that the high frequency energy has been attenuated along the travel path. The obvious place for this to occur is during the two-way transit of energy through the mantle LVZ (which also has a high anelasticity, i.e., low Q). These critical refractions are shown schematically in the ray diagram of Figure 3; we follow the convention of Archambeau et al. (1969) in labeling this cusp phase P_1.

(3) The higher frequency second arrivals for Δ< 780 km we attribute to large angle reflections from an interface lying mainly above the LVZ. These reflections are overtaken and overwhelmed by P_1 for Δ<780. Because of the apparent velocity near 8 km/s, the high frequency content, and travel time just longer than P_n, the synthetic seismogram modeling discussed below suggests this reflection occurs at the base of the mantle lid and hence our notation of P_{lid}.

Modeling

Our technique in modeling the record section was to first use a fast asymptotic ray theory computer program (Červený, 1979) to fit travel times and approximate amplitudes. For more exact modeling we then used a reflectivity method program developed by Kind (1978), which properly accounts for the effects of a buried source and thus allows computation of complete seismograms. One advantage of the reflectivity method over Cagniard-de Hoop techniques (Helmberger, 1973; Helmberger and Burdick, 1979) is that Q values can be individually assigned to each model layer rather than distributed over the entire path as part of a linear operator.

Burdick and Helmberger's (1978) T-7 model was adopted as the starting model for compressional wave velocities in the crust and mantle. The generic T-7 model was constructed mainly from long period data to the NW and SE of NTS—with emphasis on velocity structure below 200 km (arrivals for $\Delta \geq 10^o$). Since our observations are in the range $7^o < \Delta < 8^o$, we perturbed the initial model only at depths above 250 km. The T-7 model has a P_n velocity of 7.95 km/s with a positive gradient below the M-discontinuity to 8.05 km/sec at the bottom of the lid at 65 km. A substantial LVZ for P-velocities is included below 65 km (Figure 5).

We did not calculate synthetics for shear wave phases but were required to include a realistic S-velocity structure because shear wave velocity contrasts can have a major influence on P-wave reflection coefficients—especially for large angles of incidence. Priestly and Brune (1978) used dispersion of fundamental mode Rayleigh and Love waves to derive a shear velocity model in the eastern Great Basin very close to the area of the mantle turning points of this study. The combined P- and S-velocity model, T-7/PB, is shown in Figure 5 along with Poisson's ratio (σ) calculated from the tabulated velocities.

The modified reflectivity synthetics for the T-7/PB velocity model are shown in Figure 4a for an extended range from 600 km to 960 km. The P_1 phase can be seen only for distances beyond 840 km and reduced times greater than 13 seconds. In order to bring the synthetic P_1 phase into agreement with the observed arrival times and to shift the cusp from $\sim$820 km back to $\sim$780 km it was necessary to bring the gradient at the

TABLE 1. NTS Explosions of September 27, 1978

Name	Origin Time (GMT)	Coordinates Lat.	Long.	Depth (m)	Surf. Elev. (m)	Magnitude (m_b)
DRAUGHTS	1700:00.071	37.074°N	116.020°W	442	1262	5.0
RUMMY	1720:00.076	37.080°N	116.051°W	640	1253	5.7

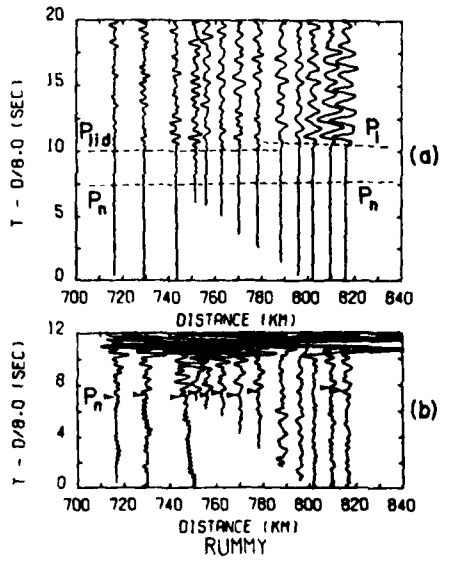

Figure 2. (a) True relative amplitude record section of P-wave arrivals from RUMMY. (b) Same as (a) with increased amplitudes to show weak P_n phase.

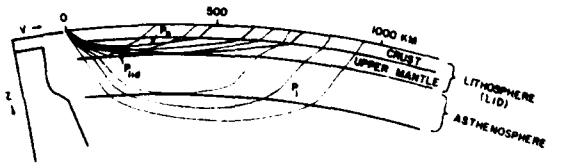

Figure 3. Schematic ray diagram showing the head wave phase P_n, the P_1 phase critically refracted from the gradient near the bottom of the LVZ, and the P_{lid} phase reflected from the base of the mantle lid.

bottom of the LVZ to shallower depths and to make slight adjustments to its curvature. Also note from Figure 4a that the T-7/PB model gives too large amplitudes for P_n arrivals, and the P_{lid} phase from the discontinuity at 65 km depth arrives about 2.5 seconds too early so is superimposed on the P_n phase throughout much of the 600-960 km range. The result of perturbing the T-7/PB velocity model to better match the observations of Figure 2 is model A-10 shown in Figure 5. The A-10 synthetics are compared with the original T-7/PB model in Figure 4b and with the more limited distance range observations in Figure 6.

Discussion

We can summarize the nature and reasons for the various model perturbations as follows:

(1) The steepened positive P-velocity gradient in the lower part of the LVZ has been raised in order to fit the arrival times and cusp distance of the P_1 phase.

(2) In order to match the observed weak P_n, a slight negative gradient just below the M-discontinuity is required instead of the positive gradient of the generic T-7 model. In fact, our A-10 P-velocity model suggests that, beneath this part of the Great Basin, the LVZ may be in contact with the crust at the M-discontinuity. Similar indications of the absence of a high velocity lid in parts of the western U.S. have been cited by Archambeau et al. (1969) (especially for their SHOAL-FALLON SE profile).

(3) The large negative discontinuity at a depth of 65 km present in both the T-7 P-velocities and the Priestly-Brune model appears to be too shallow to properly match the observed P_{lid}-P_n travel time delay. The observed delay is better reproduced if the discontinuity is at about 100 km depth.

(4) The calculated amplitudes of the P_{lid} reflection are much too large if the T-7/PB velocity

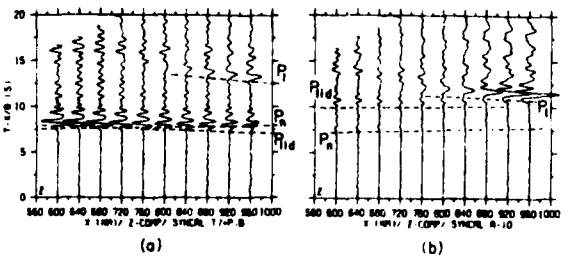

Figure 4. Synthetic seismograms (Z-component) of early compressional phase arrivals from (a) the generic T-7/PB model and (b) the A-10 mantle model (Figure 5) which match the observations in the 720 to 820-km range. Travel time curves calculated from the Cerveny program. Amplitude multiplied by distance for convenient plotting.

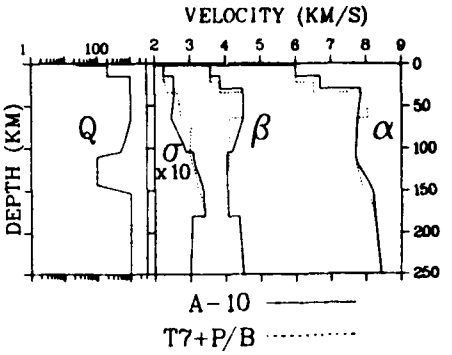

Figure 5. P-velocity (α) and S-velocity (β) versus depth plots for t[illegible] T-7/PB and A-10 models. Assumed Q-structure fo[illegible] both models shown at left. σ is Poisson's ratio.

contrasts (-0.3 km/s for P, -0.3[illegible] km/s for S) are used at a depth of ∿100 km. In fact, by including the effect of S-velocity contrasts on the P-wave reflection coefficients, we can match observed P_{lid} amplitudes by keeping the P-velocity contrast at zero and relying entirely on an S contrast of -0.15 km/s to produce the effect on these wide angle reflections. In moving the bottom of the S-velocity lid from a depth of 65 km proposed by Priestly and Brune to the ∿100 km required in our A-10 model, we introduced a negative gradient in the S-velocities between these two depths; a similar negative gradient can be seen in the higher mode inversions by Cara (1979), but these are not plotted in Figure 5. Hill (1972) and Hales (1969) previously reported arrivals following P_n by two to three seconds at distances of ∿600 km in sections from long range refraction experiments in the Columbia Plateau (EDZOE experiment) and the central U.S. (EARLY RISE), respectively. Their interpretations—using travel time information only—suggest a thin (∿10 km), sharp, but high velocity (8.0 to 8.4 km/s) lid at depths of 90-100 km is present in those regions. Our Great Basin data agrees in placing a discontinuity (which is perhaps the "boundary" between the lithosphere and the athenosphere) at ∿100 km but our P-velocity contrast cannot be as pronounced as those implied by Hill and Hales and still give rise to the comparitively weak amplitudes that we observe in the 750 km range.

(5) the Q-structure (for P-waves) used for the A-10 model was a generalization of proposed values that have appeared in recent literature. The most important segment is the low value centered in the LVZ. A Q_α value in the range between 50 and 100 appears to adequately attenuate the higher frequency components

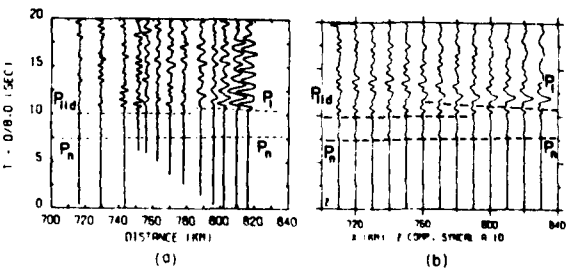

Figure 6. Comparison of observed (a) and synthetic (b) seismogram record sections for the 720 to 820-km distance range.

of the P_1 phase. $Q_\alpha > 100$ in the LVZ does not attenuate P_1 enough, whereas $Q_\alpha \sim 25$ completely obliterates the P_1 phase in the synthetics. Our value of $50<Q_\alpha<100$ is of the same order as that deduced by Helmberger (1973) from Cagniard-de Hoop techniques.

(6) One possible shortcoming of the A-10 model is the failure to reproduce details of the oscillations of the observed P_1 phase. We do not believe this to be a result of an inadequately detailed source spectrum, since a comparison of the explosion source spectrum algorithm used in the modified reflectivity code is reasonably represented by the source spectrum plus instrument response function calculated from known physical parameters of these explosions (Mueller and Murphy, 1971). Archambeau et al. (1969) observed compressional wave energy spread out in long, rather complicated oscillatory wave trains near caustics and attributed this to interference between refracted and reflected components near the cusp. Our model layer thicknesses ($\sim$5 km) in the region of the lower depths of the LVZ (120-150 km) are of the same order as the wavelengths ($\sim$10 km) of the dominant short period energy. Thus, we believe the oscillatory P_1 trains may be due to small details of fine structure in the transition zone which we have not yet attempted to model at the required resolution.

In conclusion, relatively minor adjustments in the T-7/PB model for the western U.S. yield an uppermost mantle structure that reproduces in detail the upper mantle arrivals and very weak P_n observed in the Great Basin.

Acknowledgments. We especially thank Rainer Kind for the modified reflectivity computer program used in our analysis. We appreciate the assistance of our LASL colleagues, E. F. Homuth and T. G. Handel with the observations and J. N. Stewart for computer advice. Cooperation of the Idaho National Engineering Laboratory during the field work is appreciated. K. H. O., P. A. J., and the LASL field team were supported by the U.S. Department of Energy. L. W. B. acknowledges support from NSF grants EAR-77-23351 and EAR-77-23707 and ONR grant N00014—75-C-0972. Field data were collected during research partially sponsored by the NSF grants and by USGS Geothermal Exploration Program grant 14-08-0001-G-532.

References

Archambeau, C. B., Flinn, E. A., and Lambert, D. G., Fine structure of the upper mantle, J. Geophys. Res., 74, 5825-5865, 1969.

Braile, L. W., Smith, R. B., Ansorge, J., Baker, M. R., Prodehl, C., Healy, J. H., Mueller, S., Olsen, K. H., Priestly, K., and Brune, J., The Yellowstone-Snake River Plain seismic profiling experiment: eastern Snake River Plain (abs.), EOS Trans. AGU, 60, 941, 1979.

Burdick, L. J. and Helmberger, D. V., The upper mantle P velocity structure of the western United States, J. Geophys. Res., 83, 1699-1712, 1978.

Cara, M., Lateral variations of S velocity in the upper mantle, Geophys. J. Roy. Astron. Soc., 57, 649-670, 1979.

Červený, V., Accuracy of ray theoretical seismograms, J. Geophys., 46, 135-149, 1979.

Fuchs, K. and Müller, G., Computation of synthetic seismograms with the reflectivity method and comparison with observations, Geophys. J. Roy. Astron. Soc., 23, 417-433, 1971.

Hales, A. L., A seismic discontinuity in the lithosphere, Earth and Planet. Science Letters, 7, 44-46, 1969.

Helmberger, D. V., On the structure of the low velocity zone, Geophys. J. Roy. Astron. Soc., 34, 251-263, 1973.

Helmberger, D. V. and Burdick, L. J., Synthetic seismograms, Ann. Rev. of Earth and Planetary Sciences, 7, 417-442, 1979.

Hill, D. P., Critically refracted waves in a spherically symmetric radially heterogeneous earth model, Geophys. J. Roy. Astron. Soc., 34, 251-263, 1973.

Hill, D. P., Crustal and upper mantle structure of the Columbia Plateau from long range seismic-refraction measurements, Geol. Soc. America Bulletin, 83, 1639-1648, 1972.

Johnson, L. R., Array measurements of P velocities in the upper mantle, J. Geophys. Res., 72, 6309-6323, 1967.

Kind, R., The reflectivity method for a buried source, J. Geophys. Res., 44, 603-612, 1978.

Masse, R. P., Landisman, M., and Jenkins, J. B., An investigation of the upper mantle compressional velocity distribution beneath the Basin and Range province, Geophys. J. Roy. Astron. Soc., 30, 19-36, 1972.

Mueller, R. A. and Murphy, J. R., Seismic characteristics of underground nuclear detonations: Part 1, seismic spectrum scaling, Bull. Seismol. Soc. Am., 61, 1675-1692, 1971.

Priestly, K. and Brune, J., Surface waves and the structure of the Great Basin of Nevada and Western Utah, J. Geophys. Res., 83, 2265-2272, 1978.

Romanowicz, B. A. and Cara, M., Reconsideration of the relations between S and P station anomalies in North America, Geophys. Research Letters, 7, 417-420, 1980.

Wiggins, R. A. and Helmberger, D. V., Upper mantle structure of the western United States, J. Geophys. Res., 78, 1870-1880, 1973.

York, J. E. and Helmberger, D. V., Low-velocity zone variations in the southwestern United States, J. Geophys. Res., 78, 1883-1886, 1973.

(Received September 7, 1980;
accepted October 7, 1980.)

SEISMOGRAMS OF EXPLOSIONS AT REGIONAL DISTANCES IN THE WESTERN U.S.: OBSERVATIONS AND REFLECTIVITY METHOD MODELING

K.H. Olsen
L.W. Braile

To be published in Proceedings of the NATO Advanced Study Institute:
"Identification of Seismic Sources - Earthquakes or Underground Explosion",
(Held 8-18 September 1980, Oslo, Norway)

SEISMOGRAMS OF EXPLOSIONS AT REGIONAL DISTANCES IN THE WESTERN UNITED STATES: OBSERVATIONS AND REFLECTIVITY METHOD MODELING

K. H. Olsen[1] and L. W. Braile[2]

[1] Geosciences Division, Los Alamos National Laboratory, Los Alamos, New Mexico 87545, U.S.A.
[2] Geoscience Department, Purdue University, West Lafayette, Indiana 47907, U.S.A.

ABSTRACT. Seismic energy propagating through vertically and laterally varying structures of the earth's crust and lower lithosphere-uppermost mantle is responsible for the numerous and complex seismic phases observed on short-period seismograms at regional distance ranges (100 to 2000 km). Recent advances in techniques for computing synthetic seismograms make it practical to calculate complete seismograms that realistically model many features of regional phases. A modified reflectivity method program is used to interpret some details of record sections of Nevada Test Site (NTS) underground explosions that were observed 700 to 800 km from the sources.

I. INTRODUCTION

Regional seismic phases recorded by high-gain, short-period or broadband instruments are likely to play an increasingly important role in seismic source location and identification as acceptable magnitude thresholds are pushed to lower levels. From the standpoint of complexity of seismograms, the epicentral distance range between ~200 km and the transition to simpler teleseismic waveforms around 2000 km presents many challenges to the seismic analyst. In this range, propagation paths can traverse the crust, the lower lithosphere, and the uppermost mantle where both vertical and lateral heterogeneities strongly influence waveform characteristics. Good observational data are rare for testing analysis techniques developed for regional problems. In contrast to the numerous detailed crustal refraction/reflection profiles that have been obtained from many parts of the world out to distances ~200 km, relatively few long-range

profiles exist where station spacing is sufficiently tight to facilitate a clear interpretation of the onset, development, and amplitude vs. distance behavior of the many observable phases. Thus, although signals from sources of interest may be easily observable at regional distances, derivation of source parameters from observations at sparsely located observatories or arrays will require careful analysis and modeling of the intricacies of wave propagation at these scales.

Phases of interest in regional identification studies fall into two main categories: large amplitude, long duration, but somewhat indistinct wave groups such as Lg and $\bar{P}$; and body waves (mainly compressional) that appear either as first arrivals or closely following as possible wide angle reflections/near-critical refractions from interfaces and/or steep velocity gradients in the deep crust, lower lithosphere, and uppermost mantle. The Lg and $\bar{P}$ phases are often the largest amplitude features on regional short-period seismograms, but a clear explanation of how Lg and $\bar{P}$ propagate is still lacking [1]; this lack perhaps is reflected in the fact that seismologists frequently use the notations $\bar{P}$ or P_g interchangeably in reference to a broad, large amplitude phase following P_n. We adopt the $\bar{P}$ notation here. The phase in question propagates very well in the western United States, but attenuates rapidly in the eastern U.S. A group velocity around 6 km/s implies $\bar{P}$ propagates as compressional waves multiply reflected within the crust--which may thus act as a waveguide. Similarly, the ~3.5 km/s group velocity for Lg suggests shear waves multiply reflecting within the crustal layers. Some authors [2] prefer to treat Lg as a superposition of higher mode Love and Rayleigh waves propagating in a nearly laterally homogeneous, vertically layered crust. In any case, the propagation physics is complicated and will require quite sophisticated synthetic seismogram codes to properly model and interpret observed waveforms.

Record sections of long-range seismic refraction profiles often show one or more nearly parallel travel time (T) vs. distance (Δ) branches following within several seconds of first arrivals [3, 4, 5]. Each secondary branch may be traceable only over a distance interval of 50 to 200 km before being replaced in a "shingle-like" fashion with another branch or set of arrivals [5, 6, 19]. These are usually interpreted as parts of cusp phases arising from critical refractions and/or wide-angle reflections from first order discontinuities or steep velocity gradients in the upper mantle. Archambeau et al. [7] and Burdick and Helmberger [8], for example, have derived velocity vs. depth models for the major features of the upper mantle beneath the U.S. by a joint analysis of travel times, amplitude vs. distance variations, and waveform fitting of the first few compressional arrivals observed at widely separated seismograph

stations throughout the U.S. These and similar models by others are most valid for depths greater than about 250 km. Although these analyses suggest that the main features of mantle structure at depths below about 300 km (corresponding to compressional first arrivals at epicentral ranges beyond ~1500 km) may be more uniform over a global scale [8], it is known that significant lateral variations in lower lithosphere and uppermost mantle properties occur beneath the continents on regional and perhaps even finer scales [8, 9, 10, 11]. In the depth range between the Moho and ~300 km, several types of structural variations have been suggested in the literature that would give rise to wide angle reflections, converted phases, and similar closely spaced arrivals on seismograms at regional ranges. These include the presence or absence of the S-wave and/or the P-wave low velocity zone (LVZ) in the asthenosphere, high velocity mantle lids [12, 13], alternating lamellae of positive and negative velocity gradients [6, 19], etc. These early arriving phases often have better defined onsets than the $\bar{P}$ and Lg phases and, since they are observed at distances beyond that where a true head wave Pn arrival can be expected, they may be useful in regional source location and identification. In order to make use of the information contained in these arrivals (especially the amplitude vs. distance behavior for particular paths of interest), it will be necessary to use modern sophisticated synthetic seismogram techniques to derive localized fine scale details from generalized crust-mantle models.

The purpose of this paper is to explore a few of the problems in modeling regional short-period seismograms by means of a modified reflectivity method [14] computer program developed by R. Kind [15]. This numerical program accounts for the effects of a buried source and is thus capable of computing 'complete' seismograms--including refracted waves, surface reflected body waves such as the pP phase, and surface waves. The effects of anelastic attenuation (Q) for each layer are included as an integral part of the method [15]. The most severe limitation of the technique for studies of regional seismograms is the assumption of lateral homogeneity (this is also a limitation for normal modes summation techniques). An item of interest will be the extent synthetics can be made to match observed waveforms under this restriction.

Two problems are considered. The first, labeled the B-3 model for brevity, employs a simple model consisting of three layers in the crust without velocity gradients and an almost uniform velocity mantle. A large range of apparent surface phase velocities is used in order to display S phases and surface waves. The second calculation, the A-10 model, treats the mantle structure in detail, but confines attention to compressional phases near ther start of the seismogram. The more

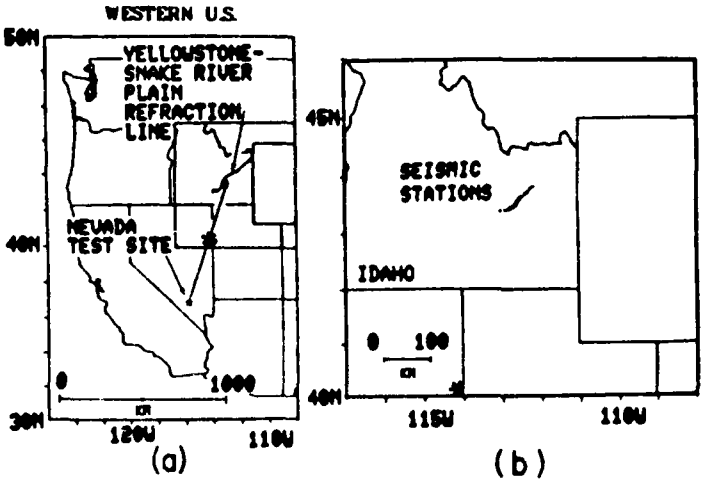

Fig. 1. (a) Location map of the western United States with relative positions of the Nevada Test Site and the Y-ESRP recording line. (b) Enlargement showing positions of stations that recorded the 27 September 1978 RUMMY explosion. Asterisk denotes approximate area for mantle ray turning points from NTS explosions.

important conclusions of the A-10 model are summarized here--a fuller discussion of this calculation and the implications for uppermost mantle structure beneath the western U.S. can be found in a previous publication [16].

A comparison of the synthetic seismogram calculations has been made with a 100-km-long record section of short-period vertical component seismograms obtained in eastern Idaho during the 1978 Yellowstone-Eastern Snake River Plains (Y-ESRP) seismic profiling experiment. For these observations, the sources were underground nuclear explosions at the Nevada Test Site (NTS) at distances between 720 and 820 km from the nearly radially oriented linear station array (Fig. 1). Only the records from the largest NTS explosion, the m_b = 5.7 RUMMY event at 1720:00.076 GMT, 27 September 1978, are reproduced here since they have the best signal-to-noise ratio of the three NTS explosions observed during the experiment. Additional details of the Y-ESRP instrumentation, experiment, and data can be found elsewhere [16].

2. COMPUTATIONAL TECHNIQUE

As discussed by Kind [15] and by Fuchs and Müller [14], the reflection coefficient and time shift calculations in the reflectivity method are carried out in the frequency domain and then Fourier transformed to plot seismograms. We included Müller's [17] earth flattening approximation in both of our problems to account for earth curvature effects. Both P and S velocities are independently specified in all calculations, since the reflection coefficients are functions of both P and S velocity contrasts at non-normal incidence angles and are required even when only computing P phases over a narrow time window. In the A-10 calculation, for example, the departure of the P/S velocity ratio in a layer from that given by Poisson's ratio = 1/4 is an important factor in our interpretation [16]. Densities are given by a Birch's Law relation (density = 0.252 + 0.3788*P velocity). The attenuation factor Q_α for P waves was chosen as 25 in the source layers, 200 in the upper crust, and 1000 in the lower crust and the uppermost mantle layers; for the LVZ modeling of the A-10 model, Q_α in the asthenospheric layers was adjusted as part of the fitting procedure (see Fig. 5). The attenuation factor for S waves was always assumed to be $4Q_\alpha/9$ [20]. The explosive source algorithm [16] was used with the source buried at a depth of 0.640 km in a layer of P velocity = 3.55 km/s. These were close to actual field values for the NTS RUMMY explosion. Time intervals, number of samples, and computed lengths of seismograms were chosen so that the dominant frequency of the source spectrum was 1.6 Hz for the A-10 calculation--again close to the observed value. In order to save computer time for the extended duration B-3 seismogram sections, the parameters were chosen so that the dominant frequency of the source was shifted to 0.25 Hz; although this was low compared to observed frequencies, we felt it was adequate for the puposes of this initial study. To avoid long computer runs, the wave field was only computed within a limited phase velocity window: 1 km/s to 20 km/s for B-3, and 6.5 km/s to 1000 km/s for A-10. These integration limits sometimes introduced spurious single cycle "phases" at these apparent velocities in the computed record sections. The limit velocities were chosen so as to not overlap or interfere with arrivals of interest in the observations. In the record section plots, the amplitudes of each trace have been multiplied by station distance to maintain a convenient scaling of the amplitudes of the phases which are subject to geometrical spreading and attenuation due to anelasticity.

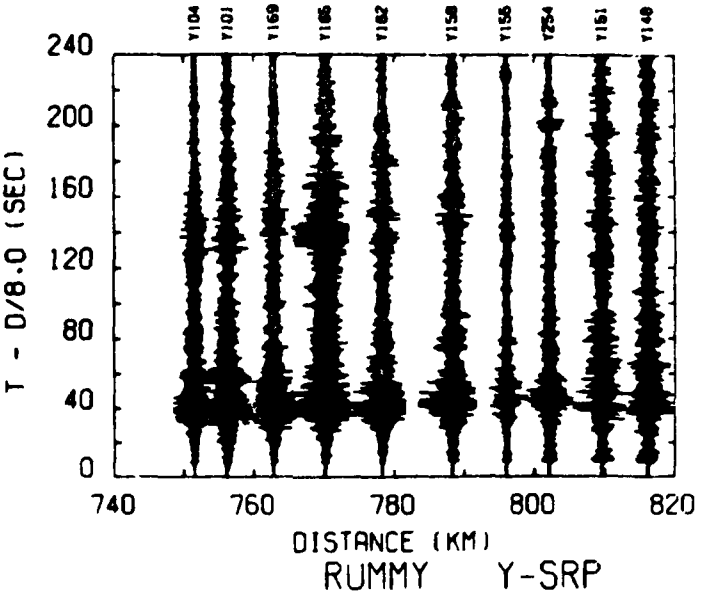

Fig. 2. Vertical component low time resolution seismic record section of the RUMMY explosion as recorded at Snake River Plains stations. The time scale is compressed to show envelope behavior; individual waveforms not readily seen. The $\bar{P}$ phase is the broad feature at reduced times between 30 and 60 s. Upward ground motion to the left.

3. DISCUSSION

3.1 The Extended Time Seismograms: B-3 Model

Figure 2 is a true relative amplitude vertical component record section of the RUMMY explosion recorded on ten matched short-period (1 Hz natural frequency) instruments deployed in the eastern Snake River Plains (Fig. 1). Although the time scale is too compressed to reveal many details of the waveforms, several important overall features can be noted. The broad (~40-second-long) envelope of the $\bar{P}$ phase appears at reduced times between approximately 30 to 60+ seconds, and is the largest amplitude feature on the record. In contrast, the Lg phase expected at reduced times of ~130+ seconds (an average velocity of about 3.5 km/s) is poorly developed on these unfiltered records; it is only obvious at the 770-km station. A few impulsive arrivals can be seen (such as the first arrivals at reduced time ~10 seconds, which will be discussed in Sec. 3.2, and perhaps an Sn [?] phase at t_{red}~80 seconds and ~780 km), but the

impression one gets by viewing this observed section is that the correlations seem to be better described as broad energy correlations rather than phase correlations. A similar conclusion is suggested by seismograms from central Asia shown in the paper of Ruzaikin et al. [1]. A coherent structure in the $\bar{P}$ and Lg phases is difficult to trace from station to station even though the stations are only separated by 8 km on the average.

The results of an attempt to model late time arrivals over a regional distance range is shown in Fig. 3. A rudimentary, almost trivial, crust/mantle velocity structure was assumed that consisted of three constant velocity layers in the crust overlaying a nearly constant velocity halfspace. (A slight negative gradient in P velocity was introduced just below the Moho in order to suppress the Pn amplitudes as required by the observations; see Sec. 3.2.) We note several points.

(a) The seismogram section from 100 to 900 km and the enlarged individual record for 800 km shows a surprising amount of complexity at times beyond the first arrivals even though an extremely simple earth model and source function is used. Groups corresponding to the $\bar{P}$ and Lg phases can be identified.

(b) There appears to be a considerable amount of S-wave energy although none is present in the explosion source algorithm. This is probably due to P-to-S and S-to-P, etc., conversions at interfaces and to multiples which the program adequately includes.

(c) The calculated dispersed fundamental mode Rayleigh wave is very large. There are at least two reasons this Rayleigh wave is not representative of the observations. First, no corrections for the short-period bandpass response of the seismometers were included in the synthetics. Second, the assumed source spectrum has too much energy at the longer periods as compared with a near point-source representative of a NTS explosion, thus over enhancing the Rayleigh waves. Long-period Rayleigh waves from actual underground explosions are probably generated or modified and enhanced by mechanisms such as spall closure and/or tectonic strain release; these mechanisms are not adequately treated by the explosion algorithm used for the present calculation.

(d) Because the calculated seismogram sections are quite complicated even for this simple earth model, they give the impression that broad "packets of energy" can be more readily correlated than any well defined phases--for at least the $\bar{P}$ and Lg phases. This was the case with the observations in Fig. 2. In order to better understand the gross behavior of these phases with distance and to identify the origin of obscure features, it will be necessary to include calculations of the horizontal

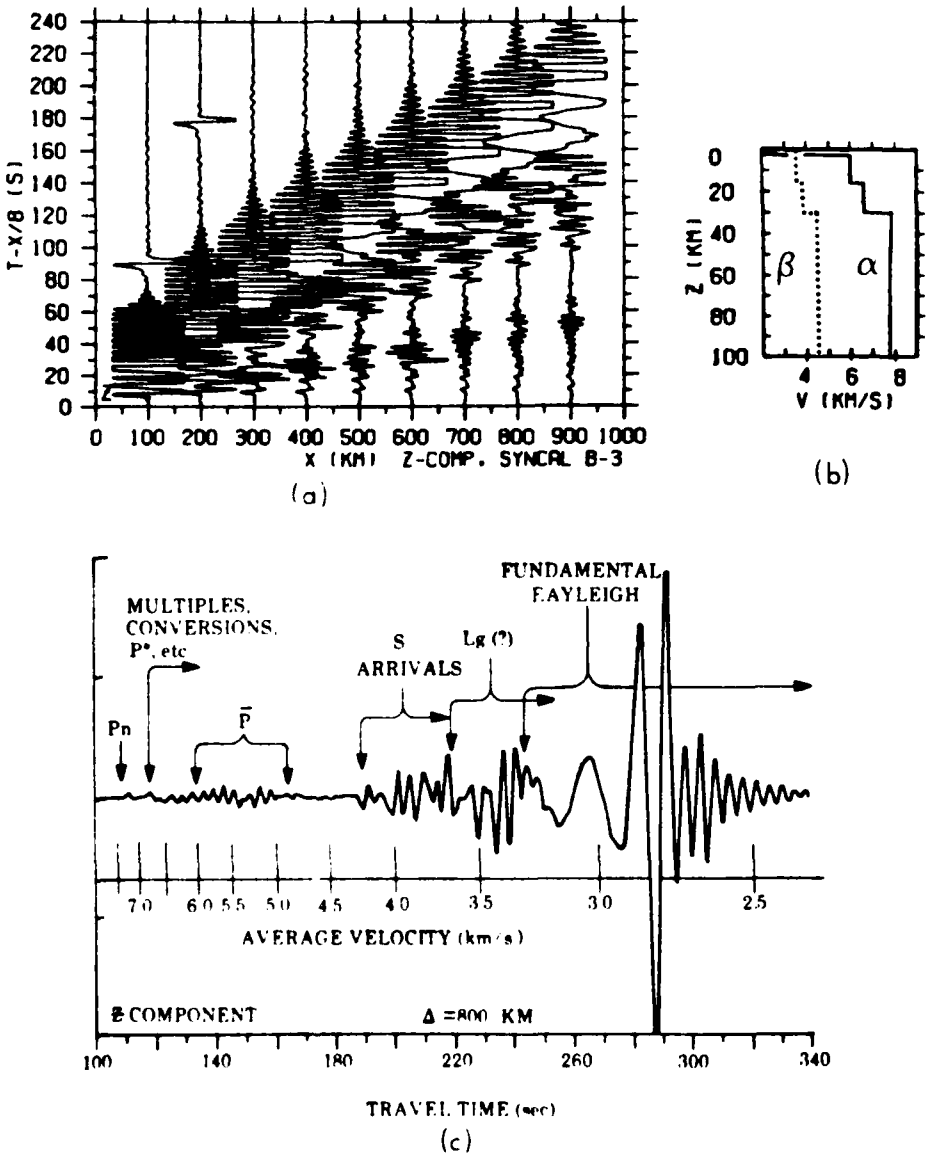

Fig. 3. (a) Synthetic seismogram vertical component record section calculated from the P and S velocity vs. depth structure (Model B-3) shown in (b). (c) Expanded plot of the synthetic seismogram at the 800-km distance. Approximate arrival time and average velocity windows for different phases or groups are indicated; the phase velocities of the different wave types are equal to or slightly greater than the average velocities. The Rayleigh waves on plot (a) are arbitrarily clipped in plotting to avoid large overlays in the seismograms.

(radial) component and to perform calculations at small station separation to increase recognizability of phase correlations.

These results suggest that the modified reflectivity method, even with the restrictive assumption of lateral homogeneity, can be a useful technique in understanding the intricacies of Lg and P phases and the types of earth structures that most affect them. In addition, these studies suggest that observations of complex and apparently-incoherent seismic phase arrivals--even over short distances--do not necessarily imply strong lateral heterogeneity in crustal structure. Parameter studies would help identify those aspects where refinements due to lateral heterogeneity and/or scattering need to be considered in order to better match observations.

3.2 Early Time Arrivals: A-10 Model

Figures 4a and 4b are enlarged portions of the first few seconds of the digitized RUMMY vertical component seismograms (see also Fig. 2) that show details of the earliest arrivals. We have interpreted [16] this record section in terms of three different compressional phases, all having apparent velocities close to 8 km/s: (a) an extremely weak leading arrival labeled Pn, which was lost in the background noise for the two other, lower yield, NTS shots that were also recorded during the Y-ESRP experiments; (b) a stronger phase labeled P_{lid} follows Pn by about two or three seconds for epicentral distances between 700 and 780 km; (c) beyond 780 km, the P_{lid} phase appears to be overtaken and overwhelmed by a low-frequency phase, P_l, whose amplitude increases rapidly with distance out to at least the farthest station of the linear array. The detailed reasons for these labels and identifications are discussed in [16]; they can be summarized as follows.

The phase labeled Pn could be a wide angle reflection from a weak P-velocity contrast in the lower lithosphere below the Moho rather than a true headwave (in the strict sense of the mathematical definition) that travels along the M-discontinuity interface over the entire 800-km path. However, the sub-Moho P velocity (7.7 to 7.9 km/s) in this region of the Great Basin is known to be close to both the average and the apparent velocity observed in Figs. 2 and 4. This, plus the fact that other travel time arguments [16] suggest there is no evidence for mantle lids or other thin but fairly high gradient zones down to a depth of about 100 km, argues that the most straightforward explanation for this arrival is that it is a P_n-type phase. We calculate that the energy at 800 km is greatly reduced because the wave travels in a region beneath the Moho that has a slight negative velocity gradient.

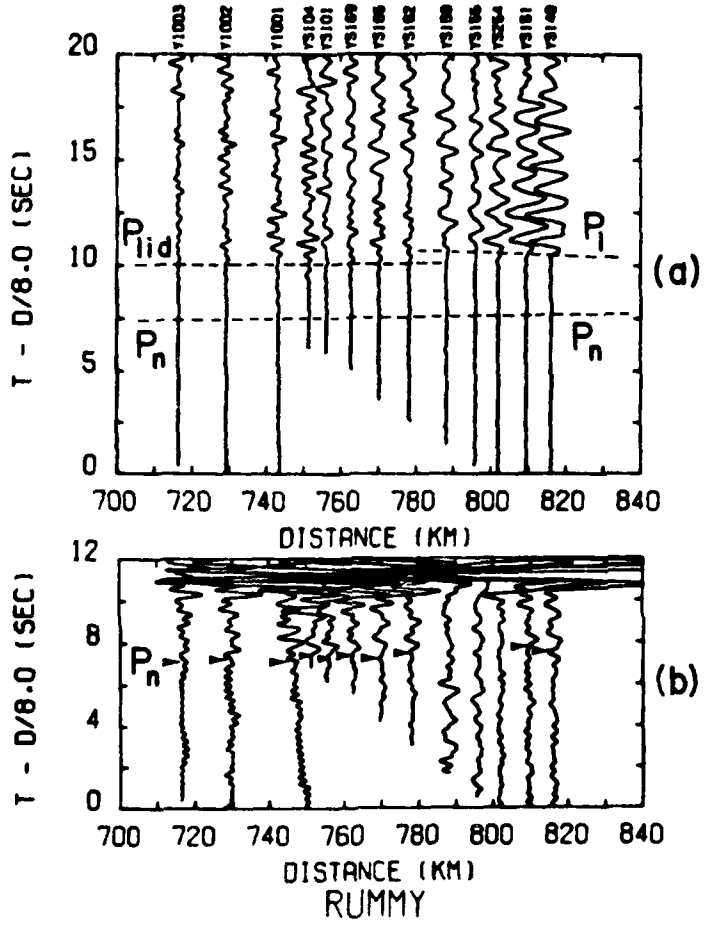

Fig. 4. (a) True relative amplitude record section of early compressional arrivals from the RUMMY explosion. (b) Same as (a) with increased amplitudes to show weak P_n phase. Upward motion to the left. All traces low pass filtered at 3 Hz.

The sudden onset at about 780 km and subsequent rapid amplitude growth of the P_l phase indicates it is the cusp of the critically refracted P-waves from the steep velocity gradient at the base of the asthenospheric low velocity zone. The observed dominant low frequency content is then explained by the attenuation of the high frequency components as the energy travels first downward and then back up through the very low-Q region of the LVZ. The notation of P_l for this phase follows the convention established by Archambeau et al. [7].

The travel times, moderate amplitudes, and relatively high frequency content imply the phase identified as P_{lid} is a wide angle reflection from a discontinuity near the base of the mantle lid (= top of LVZ) in this area.

The conclusions concerning these three early arriving compressional phases summarized above were confirmed by using the modified reflectivity program to quantitatively model the arrival times, amplitudes, and waveforms in the first 15 seconds of the record sections. The procedure was to begin with a generic P-velocity vs. depth model for the western U.S. (the T-7 model) derived from a wider data set by Burdick and Helmberger [8] and then to perturb the model to achieve a better fit [16]. Because of the influence of S-velocity contrasts on the P-wave reflectivity calculations, an S-velocity vs. depth model derived by Priestly and Brune [18] from an analysis of Rayleigh and Love wave dispersion on paths crossing the area of interest in the Great Basin of Eastern Nevada was incorporated into the synthetic seismogram modeling. The starting T-7 and Priestly-Brune (P/B) velocity models are shown by dotted lines in Fig. 5. The generic T-7 P-wave model has a pronounced mantle lid with a strong positive P-velocity gradient beneath the Moho for depths from 33 to 65 km. Calculation of synthetics for this lid structure gave very large amplitudes for the "P_n" arrival, which was superimposed on a strong reflection from the base of the lid at 65 km [16]. Thus, the T-7 + P/B starting model gave results very different from observations. However, as seen in Fig. 5, only small changes to the initial model were necessary to match the observations. To bring the calculated synthetic seismograms into agreement with observations, the gradient at the base of the LVZ had to be raised to shallower depths and the positive gradient lid replaced with a smooth but gradual negative gradient starting at the M-discontinuity. The final model, A-10, that matches observations is shown by the solid lines in Fig. 5. Figure 6 is the comparison between the observed and synthetic record sections. Interestingly, no discontinuity in P-velocity is necessary to explain the P_{lid} reflections; the reflections can be adequately modeled by a small negative step in S velocities at a depth of about 100 km. The synthetics, however, do not seem to adequately model the long oscillatory trains following the P_1 phase onset. This is probably due to interference effects caused by fine structure in the lower LVZ velocity gradient that we have not yet modeled by thin enough layers in the calculation [16].

These calculations illustrate that synthetic modeling techniques can be helpful in phase identification and in quantitative calculations of amplitude vs. distance behavior and waveform characteristics. With a sophisticated reflectivity method calculation we were able to model several important features of

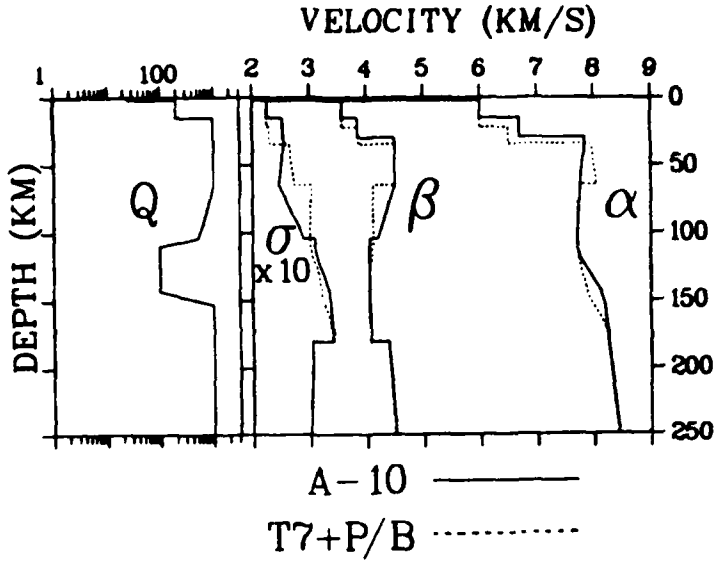

Fig. 5. P-velocity (α) and S-velocity (ß) vs. depth plots for the T-7/Priestly-Brune and A-10 models. Assumed Q structure at left: σ (dimensionless) is Poisson's ratio.

regional short-period seismograms. The technique appears promising in advancing knowledge of wave propagation and source identification at regional distance ranges.

ACKNOWLEDGMENTS

We especially thank Rainer Kind for making available to us the modified reflectivity method computer program that we have adapted for our analyses. Paul A. Johnson was responsible for the computer runs. We thank Terry C. Wallace and Mike Shore for discussions and for reviewing the manuscript. The calculational and data reduction efforts for this research were supported by the U.S. Department of Energy and partially by ONR Earth Physics Program grant N00014-75-C-0972 to L.W.B. The Snake River Plains data were collected during research partially funded by the U.S. National Science Foundation (grant EAR-77-23707 to the University of Utah and EAR-77-23357 to Purdue University) and by the U.S.G.S. Geothermal Research Program grant 14-08-0001-G-532 to Purdue.

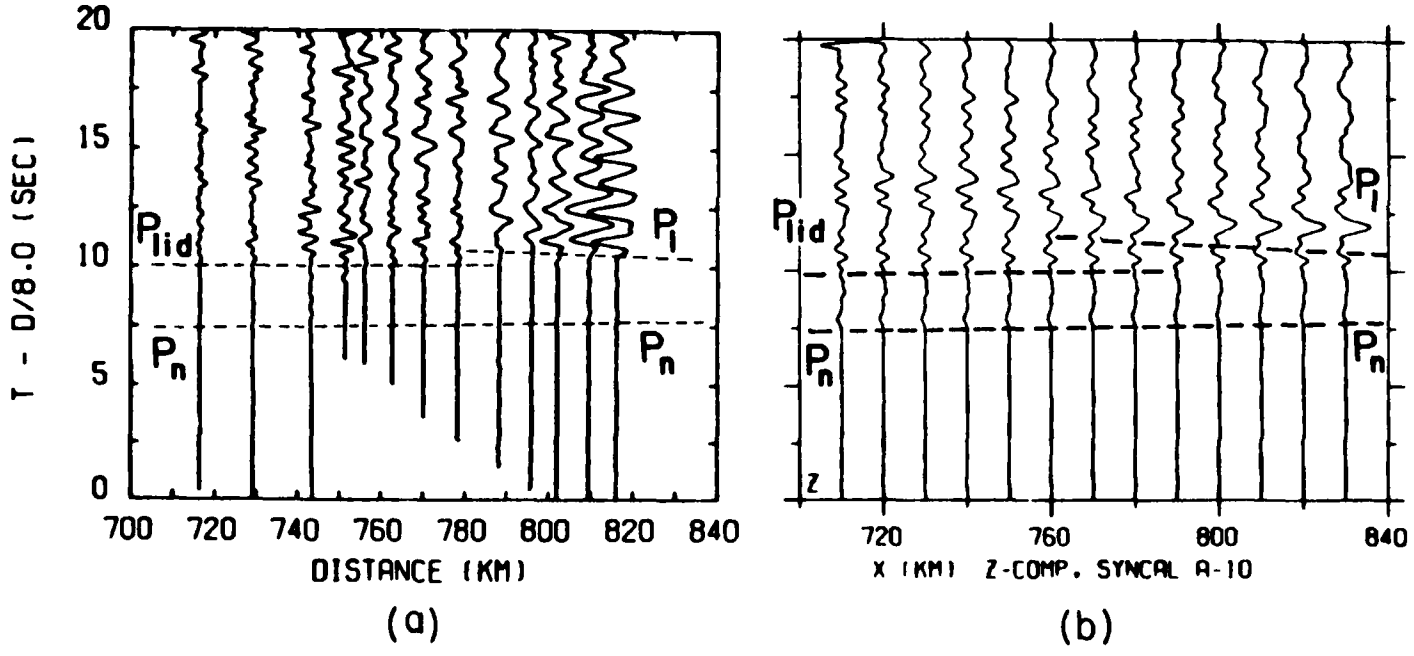

Fig. 6. Comparison of the observed (a) record section with the synthetic section calculated from the A-10 model (b).

REFERENCES

1. A. I. Ruzaikin, I. L. Nersesov, V. I. Khalturin, and P. Molnar, J. Geophys. Res. 82, pp. 307-316, 1977.
2 L. Knopoff, F. Schwab, K. Nakanishi, and F. Chang, Geophys. J. R. Astr. Soc. 39, pp. 41-70, 1974.
3. V. Z. Ryaboi, Izv. (Bull.) Acad. Sci. USSR, Geophys. Ser., AGU Trans. 3, pp. 177-184, 1966.
4. R. P. Masse, Bull. Seism. Soc. Am. 63, pp. 911-935, 1973.
5. A. Hirn, L. Steinmetz, R. Kind, and K. Fuchs, Z. Geophys. 39, pp. 363-384, 1973.
6. R. Kind, J. Geophys. 40, pp. 189-202, 1974.
7. C. B. Archambeau, E. A. Flinn, and D. G. Lambert, J. Geophys. Res. 74, pp. 5825-5865, 1969.
8. L. J. Burdick and D. V. Helmberger, J. Geophys. Res. 83, pp. 1699-1712, 1978.
9. J. E. York and D. V. Helmberger, J. Geophys. Res. 78, pp. 1883-1886, 1973.
10. M. Cara, Geophys J. R. Astr. Soc. 57, pp. 649-670, 1979.
11. B. A. Romanowicz and M. Cara, Geophys. Res. Lett. 7, pp. 417-420, 1980.
12. A. L. Hales, Earth and Planet. Sci. Lett. 7, pp. 44-46, 1969.
13. D. P. Hill, Geol. Soc. Am. Bull. 83, pp. 1639-1648, 1972.
14. K. Fuchs and G. Müller, Geophys. J. R. Astr. Soc. 23, pp. 417-433, 1971.
15. R. Kind, J. Geophys. 44, pp. 603-612, 1978.
16. K. H. Olsen, L. W. Braile, and P. A. Johnson, Geophys. Res. Lett. 7, pp. 1029-1032, 1980.
17. G. Müller, J. Geophys. 42, pp. 429-436, 1977.
18. K. Priestly and J. Brune, J. Geophys. Res. 83, pp. 2265-2272.
19. K. Fuchs, Tectonophysics 56, pp. 1-15, 1979.
20. L. Knopoff, Rev. Geophys. 2, pp. 625-660, 1964.

DISTRIBUTION LIST

Chief of Naval Research
Department of the Navy
800 North Quincy Street
Arlington, Virginia 22217
Code 100C1 (1)
Code 460 (1)
Code 463 (5)
Code 480 (1)

ONR Resident Representative
Ohio State Univ. Research Center
1314 Kinnear Road
Columbus, OH 43212 (1)

Director
Naval Research Laboratory
Code 2627
Washington, DC 0375 (6)

Office of Research, Development, Test, and Evaluation
Department of the Navy
Code NOP-987J
Washington, DC 20350 (1)

Director
Defense Advanced Research
Projects Agency
1400 Wilson Boulevard
Arlington, Virginia 22209 (1)

Air Force Office of
Sciencific Research
Department of the Air Force
Directorate of Physics (MPG)
Building 410
Bolling Air Force Base
Washington, DC 20332 (1)

Army Research Office
Department of the Army
Geosciences Division
Box 12211
Research Triangle Park,
North Carolina 27709 (1)

Defense Documentation Center
Building 5
Cameron Station
Alexandria, Virginia 22314 (12)

Procuring Contracting Officer, Code 613
Office of Naval Research
Department of the Navy
800 N. Quincy Street
Arlington, Virginia 22217 (1)

SUPPLEMENTARY DISTRIBUTION LIST

Division of Sponsored Programs (1)
Purdue University
West Lafayette, IN 47907

Prof. James Dorman (1)
Galveston Geophysics Lab of
Marine Science Inst.
University of Texas
Marine Science Inst.
Austin, TX 78712

Dr. George Sutton (1)
Dept. of Geology & Geophysics
University of Hawaii
Honolulu, Hawaii 96822

Dr. Gary Latham (1)
Galveston Geophysics Lab of
Marine Science Inst.
University of Texas
Marine Science Inst.
Austin, TX 78712

Dr. John Kuo (1)
Henry Krumb School of Mines
Columbia University
New York, New York 10027

Dr. Mark Odegard (1)
Earth Physics Program, Code 463
Office of Naval Research
Arlington, VA 22217

Dr. Robert E. Houtz (1)
Lamont-Doherty Geological Obs.
Columbia University
New York, New York 10029

Dr. John G. Heacock (1)
Earth Physics Program, Code 463
Office of Naval Research
Arlington, VA 22217


DATE
ILME